Epitaxial Films

DOI: 10.1002/anie.200905804

Facile Chemical Solution Deposition of High-Mobility Epitaxial Germanium Films on Silicon**

Guifu Zou, Hongmei Luo, Filip Ronning, Baoquan Sun,* Thomas M. McCleskey, Anthony K. Burrell, Eve Bauer, and Q. X. Jia**

The high carrier mobility and large absorption coefficient at near-infrared wavelengths[1–5] make germanium one of the most attractive semiconductor materials for a wide range of applications.[6–9] For example, the small band gap makes Ge a candidate for photodetectors and modulators at wavelengths in the range 1.3–1.6 μm. The high carrier mobility makes Ge the choice for high-speed transistors, which have potential applications in computers and switching systems. For many applications, the growth of Ge on Si is necessary. Different techniques have been used to grow Ge films on Si substrates.[10–12] Unfortunately, the large capital investment, complicated processes, and a relatively small area coating have limited wide applications of these systems. Moreover, a thick buffer layer is generally required if a relaxed epitaxial Ge film is grown on Si.[10,13,14] We have grown epitaxial Ge films on Si substrates for the first time by a cost-effective chemical solution deposition method initially developed for the growth of metal oxide films.[15] Our films are fully relaxed without the use of a buffer layer. Hall mobility values of the Ge films of up to 1700 $cm^2 V^{-1} s^{-1}$ were attained at room temperature. Furthermore, we have integrated Ge with wide-band-gap ZnO nanoparticles and demonstrated a photovoltaic response from this heterostructure.

It is well known that both Ge and Si crystallize in the diamond structure. The relatively small lattice mismatch (ca. 4.17%; $a_{Ge} = 5.6576$ Å; $a_{Si} = 5.4309$ Å) makes it possible to grow Ge epitaxially on Si. Figure 1 shows the X-ray diffraction (XRD) 2θ scan, (004) rocking curve, and (202) ϕ scans of a Ge film on Si. As can be seen from Figure 1a, there are only (004) peaks from the Ge film and Si substrate. This fact indicates that Ge is preferentially oriented along the *c* axis perpendicular to the substrate surface. A value of 0.34° for the full width at half maximum (FWHM) of the (004) rocking curve (Figure 1b) of Ge, in comparison with a value of 0.15° for the single-crystal Si substrate, indicates good crystallinity of the Ge film. The in-plane orientation between the Ge film and the Si substrate is determined by XRD ϕ scans from (202) Ge and (202) Si, respectively (Figure 1c). An average FWHM value of 1.2° for the Ge film, as compared with a value of 0.5° for the Si substrate, indicates good epitaxial quality. The heteroepitaxial relationships between the Ge film and the Si substrate, based on Figure 1, can be described as $(001)_{Ge}||(001)_{Si}$ and $[202]_{Ge}||[202]_{Si}$.

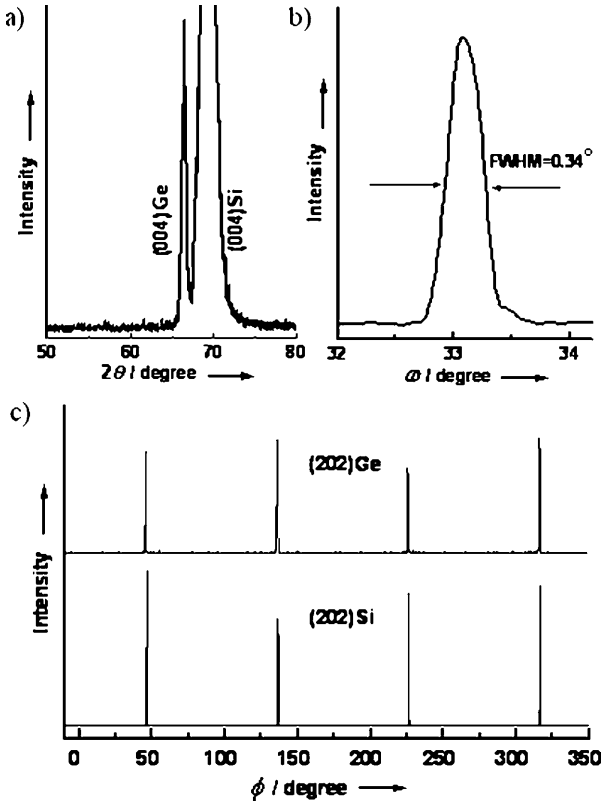

Figure 1. XRD patterns of a Ge film on a (001) Si substrate. a) θ–2θ scan. b) Rocking curve from Ge (004) reflection. c) ϕ-scans from (202) reflections of both Ge film and Si substrate.

The surface morphologies of the Ge film were characterized by the atomic force microscopy (AFM). As shown in Figure 2a,b, a uniform surface with a homogeneous grain size of around 80 nm was observed across a scan area of 5×5 μm^2. The root-mean-squared (rms) surface roughness of a 25 nm thick Ge layer is around 3 nm. Figure 2c,d shows bright-field

[*] G. Zou, F. Ronning, T. M. McCleskey, A. K. Burrell, E. Bauer, Q. X. Jia
Materials Physics and Applications Division, Los Alamos National Laboratory
Los Alamos, NM 87545 (USA)
E-mail: gfzou@lanl.gov
qxjia@lanl.gov
H. Luo
Department of Chemical Engineering, New Mexico State University
Las Cruces, NM 88003 (USA)
B. Q. Sun
Functional Nano and Soft Materials Laboratory, Soochow University
199 Ren'ai Road, Suzhou 215123 (China)
E-mail: bqsun@suda.edu.cn

[**] We gratefully acknowledge the support of the US Department of Energy through the LANL/LDRD program and the Center for Integrated Nanotechnologies (CINT) for this work. B.Q.S. thanks the National Natural Science Foundation of China (Grant No. 60976050) for support.

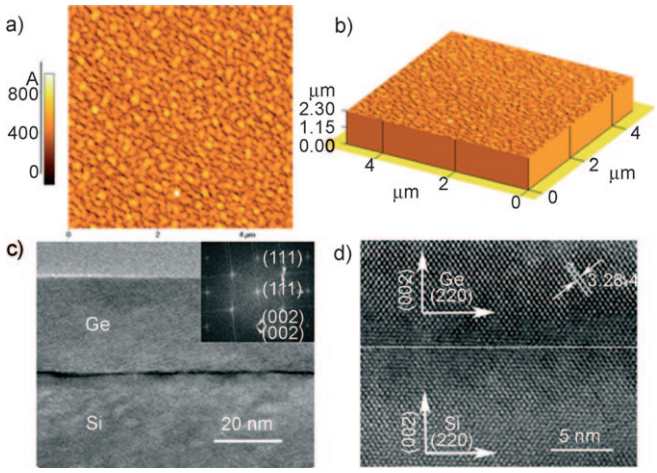

Figure 2. AFM images showing the surface morphology (a) and three dimensional topology (b) of the epitaxial Ge films. Low-magnification (c; inset shows FFT patterns of Ge and Si) and high-resolution TEM images (d) of the interface microstructure between the epitaxial Ge film and the Si substrate.

cross-sectional transmission electron microscopy (TEM) and high-resolution TEM (HRTEM) images. The bright-field image indicates that the interface between the Ge film and the Si substrate is flat. The corresponding fast Fourier transform (FFT) patterns taken from the interface (inset in Figure 2c) confirm the epitaxial growth of the Ge film on the Si substrate, as evidenced by the distinct diffraction spots from the film and the substrate. The epitaxial relationships between the Ge film and the Si substrate determined from the FFT patterns is consistent with those determined from the XRD patterns. The lattice parameter of such an epitaxial Ge film calculated from the HRTEM imaage (shown in Figure 2d) is 0.567 nm, which is in agreement with a value of 0.566 nm calculated from the XRD measurement. The very small difference in lattice parameters (within the measurement error) between the bulk and the film indicates that our epitaxial Ge film is relaxed.

A thick or graded buffer between Ge and Si is normally required to obtain relaxed epitaxial Ge films on Si substrates.[16–18] For example, a relaxed GeSi buffer layer can be deposited on Si at the expense of creating misfit dislocations, and relaxed Ge is deposited thereafter on GeSi.[19,20] In comparison, our Ge films are relaxed even though they are deposited directly on Si substrates. We believe that the use of polymer in the precursor plays an important role in the formation of relaxed Ge films. It is known that very strong local strain fields can be formed around the individual carbon atoms.[21] The dislocation glide requires a higher energy in the interface of Ge/Si containing carbon atoms.[22] It has been suggested that the ternary Ge/Si/C system should be considered as a new material with its own strain degree and relaxation behavior rather than like a Ge/Si film with an artificially reduced strain.[23] In our process, carbon atoms are present from the decomposition of polyethyleneimine (PEI) and ethylenediaminetetraacetate (EDTA) at high temperature.[15,24] This was observed in our previous nitride films as well.[25] We should treat our Ge on Si as a ternary Ge/Si/C system instead of a conventional binary Ge/Si system. In this case, carbon helps the relaxation of Ge on Si, which has also been observed in the buffered structure containing carbon atoms.[26]

The transport properties of Ge films were investigated by a standard four-probe technique. Figure 3 shows the resistivity, electron mobility, and carrier concentration of a Ge film

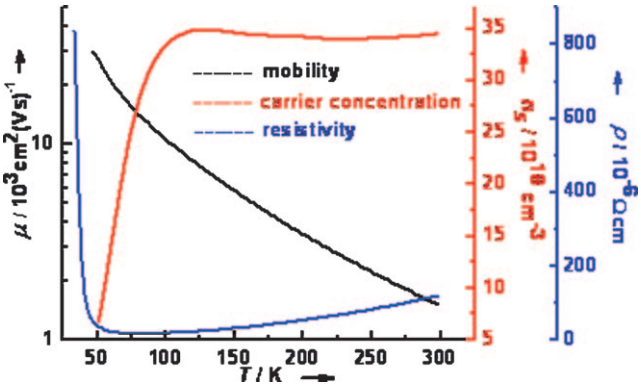

Figure 3. Transport properties of epitaxial Ge films: Temperature-dependent resistivity (ρ), mobility (μ), and carrier concentration (n_s) of an epitaxial Ge film on a Si substrate.

on Si as a function of temperature. A broad range of minimum resistivity suggests pure Ge films were obtained.[27] It is well known that the electron mobility is largely affected by defects.[28] It can be reduced by as much as two orders of magnitude when dislocations exceed certain levels.[29] As shown in Figure 3, the Hall mobility of our Ge films can reach up to 1700 $cm^2 V^{-1} s^{-1}$ for a carrier concentration of 3.45×10^{19} cm^{-3} at room temperature. As a comparison, our Ge films prepared through chemical solution deposition show electron mobility as good as the Ge films prepared by some physical vapor techniques.[30–32]

We further explored the photovoltaic response by forming a heterojunction of Ge on ZnO nanocrystals (NCs) using our chemical solution method to deposit Ge films. The device structure is illustrated in Figure 4a. By forming a heterojunction between Ge and ZnO, one would expect to observe a photovoltaic effect from this prototype device. As shown in Figure 4b, the conduction band offset ($\Delta E_c = \chi_{ZnO} - \chi_{Ge}$) between ZnO and Ge is small. However, the valence band offset ($\Delta E_v = (\chi_{Ge} + E_{GGe}) - (\chi_{ZnO} + E_{GZnO})$) is quite large ($\chi$ and E_G are the electron affinity and energy band gap, respectively). The electrons in Ge are depleted near the Ge/ZnO interface, but under accumulation in ZnO. In other words, Ge is favorable to transfer electrons to ZnO, and holes from ZnO to Ge. In addition to charge transfer, Förster exciton transfer could be expected to occur as well, since this energy transfer does not require wavefunction overlap (tunneling) between these two materials.[33]

Figure 5a shows the short-circuit external quantum efficiency (EQE) of Ge on ZnO NCs as a function of wavelength. To gain a better understanding of the experimental results, we also measured the absorption spectra of pure ZnO and Ge films (bottom panel of Figure 5a). As can be seen from the

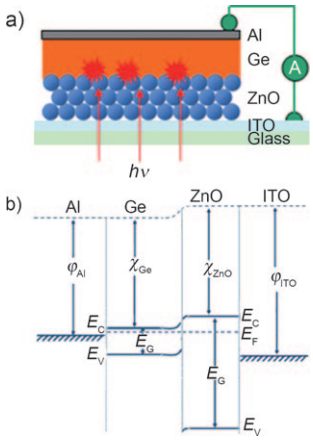

Figure 4. a) Schematic of a Ge/ZnO heterojunction structure comprising a Ge film on ZnO NCs (not to scale). b) Energy-band diagram of that system.

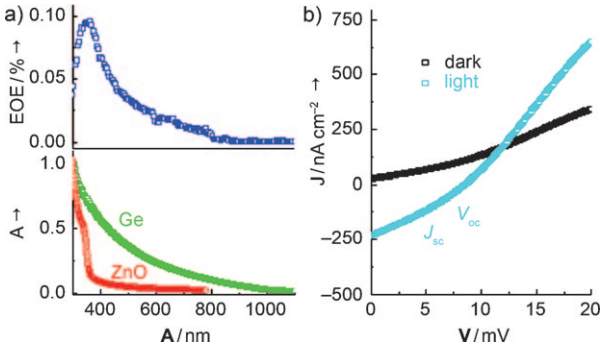

Figure 5. Photovoltaic response of a Ge/ZnO heterojunction. a) Short-circuit EQE of the heterojunction (top panel), and the absorption spectra of pure Ge and ZnO films (bottom panel). b) The *J*–*V* characteristic of the device in the dark and under illumination from an unfiltered xenon lamp.

EQE spectrum, the device shows a broad range of light response ranging from 350 nm to 800 nm. The EQE at low energies (wavelength > 400 nm) mimics the spectral shape of Ge absorption, indicating that the photocurrent in this spectral range is primarily from the Ge. For wavelengths shorter than around 400 nm, the EQE spectrum deviates from that of the Ge absorption spectrum, which is a direct indication of charge contribution from ZnO. In other words, both ZnO and Ge contribute to the photocurrent at wavelengths under 400 nm. Theoretically, larger EQE values could be achieved if the photogenerated charges can be collected. Nevertheless, our present EQE value is quite low. Charge recombination can be a limiting factor to achieve large EQE values. The smaller carrier mobility of Ge films (on ITO/glass) can also contribute to the much lower EQE value, since the Ge/ZnO film was annealed at much lower temperature (500 °C) than when Si is used as the substrate (900 °C). We also tested the current charge density versus voltage (*J*–*V*) characteristics by illuminating the device with white light from a 5 mW cm^{-2} xenon lamp. Figure 5b shows the *J*–*V* curves with and without illumination. An open-circuit voltage (V_{oc}) of 9.2 mV and a short-circuit current density (J_{sc}) of 240 nA cm^{-2} were clearly demonstrated. Although the absolute values are still small, optimizing the annealing temperature to enhance the quality of Ge should improve the device performance. For example, one can use quartz, instead of glass, as the substrate so that higher annealing temperatures can be used. More efforts are underway to optimize the processing conditions to achieve better performance.

In summary, we have demonstrated polymer-assisted deposition as a facile and cost-effective approach to the growth of epitaxial Ge films on Si substrates. Structural analysis shows high-crystallinity films with desirable surface and interface properties are produced. The Hall mobility of our Ge films can reach up to 1700 cm^2 V^{-1} s^{-1} for a carrier concentration of 3.45×10^{19} cm^{-3} at room temperature. We further explored the photovoltaic response by forming a heterojunction of Ge on ZnO nanocrystals. Our proof-of-principle device demonstrates the feasibility of combining two different materials with complimentary functionalities for improved properties through a simple and inexpensive chemical solution method.

Experimental Section

Precursor solution preparation: The solution was made by adding EDTA (2.5 g; Aldrich 99.995 %) to 25 mL water purified to 18 MΩ cm. High-purity GeO_2 (1.26 g; 99.99 %) was added to the solution, followed by the addition of PEI (4 g). The solution was subjected to ultrafiltration through Amicon stirred cells and a 10000 molecular weight cutoff ultrafiltration membrane under 60 psi argon pressure. Metal analysis showed the final concentration of the Ge solution to be 175 mM Ge.

Film preparation: Si(001) substrates were cleaned to remove organic residues from the surface by a 3:1 mixture of concentrated H_2SO_4 with H_2O_2 for 10 min, and then rinsed with deionized water. Additionally, the Si(001) substrates were etched for 30 min in 40 % NH_4F and rinsed in deionized water. Finally, the precursor solution was spin-coated on Si at 2500 rpm for 20 s. The films were annealed in forming gas at 900 °C for 3 h. Films with thickness in the range 25–35 nm were obtained from one spin-coat. Thicker films could be deposited by increasing the concentration of Ge and by multiple spin-coats.

Photovoltaic hybrid structure based on a Ge film: Colloidal ZnO NCs capped with acetate were synthesized from zinc acetate and potassium hydroxide in methanol as described in our previous report.[34] After the NCs settled out from the methanol solvent, the precipitate was washed with methanol. The NCs was redispersed into chloroform/methanol (1:3, v/v) with a concentration of 50 mg mL^{-1}. The ZnO NCs are spherical and have a diameter of (6 ± 1.5) nm as determined by TEM.

The glass substrates coated with ITO were washed sequentially in acetone and 2-propanol, and then treated by oxygen plasma to get rid of any residual organic compounds. ZnO NC films were obtained by spin-coating onto an ITO/glass substrate. The thickness of the NC films was approximately 140 nm. Ge films were then grown on the ZnO NCs films by a similar process as above except an annealing temperature of 500 °C was used. For the photovoltaic measurements, aluminum electrodes were patterned by a shadow mask with an area of approximately 2 mm^2.

Characterization: The Ge concentration in the precursor solution was evaluated by inductively coupled plasma/atomic emission spectrometry. X-ray diffraction (XRD) was used to characterize the crystallographic orientation of the films. The surface morphology and surface roughness of the films were analyzed by scanning electron microscopy and atomic force microscopy. The microstructure of the

films was further analyzed by transmission electron microscopy. The Hall mobility was measured from 30–300 K using the Van der Pauw technique. Absorption spectra were acquired by a spectrophotometer. Monochromatic illumination was provided by a 150 W xenon lamp dispersed by a monochromator. The power intensity was determined by a calibrated silicon diode. Current–wavelength and current–voltage curves were obtained by Keithley measurement units.

Received: October 15, 2009
Revised: January 7, 2010
Published online: February 5, 2010

Keywords: germanium · mobility · solution deposition · thin films

[1] W. C. Dunlap, *Science* **1950**, *112*, 419 – 420.
[2] Y. H. Kuo, Y. K. Lee, Y. Ge, S. Ren, J. E. Roth, T. I. Kamins, D. A. B. Miller, J. S. Harris, *Nature* **2005**, *437*, 1334 – 1336.
[3] J. Xiang, A. Vidan, M. Tinkham, R. M. Westervelt, C. M. Lieber, *Nat. Nanotechnol.* **2006**, *1*, 208 – 213.
[4] F. P. Bundy, J. S. Kasper, *Science* **1963**, *139*, 340 – 341.
[5] G. Lucovsky, R. F. Schwarz, R. B. Emmons, *J. Appl. Phys.* **1964**, *35*, 622 – 628.
[6] L. Colace, G. Masini, G. Assanto, *IEEE J. Quantum Electron.* **1999**, *35*, 1843 – 1852.
[7] J. Xiang, W. Lu, Y. J. Hu, Y. Wu, H. Yan, C. M. Lieber, *Nature* **2006**, *441*, 489 – 493.
[8] G. Bajor, K. C. Cadien, M. A. Ray, J. E. Greene, P. S. Vijayakumar, *Appl. Phys. Lett.* **1982**, *40*, 696 – 699.
[9] B. Ferland, C. Akyuz, A. Zaslavsky, T. Sedgwick, *Phys. Rev. B* **1996**, *53*, 994 – 997.
[10] J. C. Bean, *Science* **1985**, *230*, 127 – 131.
[11] L. Colace, G. Masini, G. Assanto, H. C. Luan, K. Wada, L. C. Kimerling, *Appl. Phys. Lett.* **2000**, *76*, 1231 – 1233.
[12] B. W. Sloope, C. O. Tiller, *J. Appl. Phys.* **1962**, *33*, 3458 – 3463.
[13] Y. B. Bolkhovityanov, A. S. Deryabin, A. K. Gutakovskii, A. V. Kolesnikov, L. V. Sokolov, *Semiconductors* **2007**, *41*, 1234 – 1239.
[14] K. Said, J. Poortmans, M. Caymax, J. F. Nijs, L. Debarge, E. Christoffel, A. Slaoui, *IEEE Trans. Electron Devices* **1999**, *46*, 2103 – 2110.
[15] Q. X. Jia, T. M. Mccleskey, A. K. Burrell, Y. Lin, G. E. Collis, H. Wang, A. D. Q. Li, S. R. Foltyn, *Nat. Mater.* **2004**, *3*, 529 – 532.
[16] F. K. LeGoues, B. Meyerson, J. F. Morar, *Phys. Rev. Lett.* **1991**, *66*, 2903 – 2906.
[17] Y. H. Xie, D. Monroe, E. A. Fitzgerald, P. J. Silverman, F. A. Thiel, G. P. Watson, *Appl. Phys. Lett.* **1993**, *63*, 2263 – 2264.
[18] J. L. Liu, C. D. Moore, G. D. U′Ren, Y. H. Luo, Y. Lu, G. Jin, S. G. Thomas, M. S. Goorsky, K. L. Wang, *Appl. Phys. Lett.* **1999**, *75*, 1586 – 1588.
[19] E. A. Fitzgerald, Y. H. Xie, M. L. Green, D. Brasen, A. R. Kortan, J. Michel, Y. J. Mii, B. E. Weir, *Appl. Phys. Lett.* **1991**, *59*, 811 – 813.
[20] J. Tersoff, *Appl. Phys. Lett.* **1993**, *62*, 693 – 695.
[21] B. Dietrich, H. J. Osten, H. Rucker, M. Methfessel, P. Zaumseil, *Phys. Rev. B* **1994**, *49*, 17185 – 17190.
[22] H. J. Osten, J. Klatt, *Appl. Phys. Lett.* **1994**, *65*, 630 – 632.
[23] H. J. Osten, D. Endisch, E. Bugiel, B. Dietrich, G. G. Fischer, M. Kim, D. Kruger, P. Zaumseil, *Semicond. Sci. Technol.* **1996**, *11*, 1678 – 1687.
[24] A. K. Burrell, T. McCleskey, Q. X. Jia, *Chem. Commun.* **2008**, 1271 – 1277.
[25] H. M. Luo, H. Wang, Z. Bi, G. F. Zou, T. M. McCleskey, A. K. Burrell, E. Bauer, M. E. Hawley, Y. Wang, Q. X. Jia, *Angew. Chem.* **2009**, *121*, 1518 – 1521; *Angew. Chem. Int. Ed.* **2009**, *48*, 1490 – 1494.
[26] H. J. Osten, E. Bugiel, P. Zaumseil, *Appl. Phys. Lett.* **1994**, *64*, 3440 – 3442.
[27] P. P. Debye, E. M. Conwell, *Phys. Rev.* **1954**, *93*, 693 – 706.
[28] K. Ismail, *J. Vac. Sci. Technol. B* **1996**, *14*, 2776 – 2779.
[29] H. J. Osten, E. Bugiel, *Appl. Phys. Lett.* **1997**, *70*, 2813 – 2815.
[30] D. Reinking, M. Kammler, M. Horn-von Hoegen, K. R. Hofmann, *Appl. Phys. Lett.* **1997**, *71*, 924 – 926.
[31] P. O. Hansson, J. H. Werner, L. Tapfer, L. P. Tilly, E. Bauser, *J. Appl. Phys.* **1990**, *68*, 2158 – 2163.
[32] D. Reinking, M. Kammler, M. Horn-von Hoegen, K. R. Hofmann, *Jpn. J. Appl. Phys. Lett.* **1997**, *36*, L1082 – L1084.
[33] J. R. Lakowicz, *Principles of Fluorescence Spectroscopy*, 2nd ed., Kluwer/Plenum, New York, **1999**.
[34] B. Q. Sun, H. Sirringhaus, *J. Am. Chem. Soc.* **2006**, *128*, 16231 – 16237.

